Variable Range Hopping Conduction in Semiconductor Nanocrystal Solids

Dong Yu, Congjun Wang, Brian L. Wehrenberg, and Philippe Guyot-Sionnest
James Franck Institute, University of Chicago, Chicago, Illinois 60637, USA
(Received 22 December 2003; published 25 May 2004)

The temperature and electrical field dependent conductivity of *n*-type CdSe nanocrystal thin films is investigated. In the low electrical field regime, the conductivity follows $\sigma \sim \exp[-(T^*/T)^{1/2}]$ in the temperature range $10 < T < 120$ K. At high electrical field, the conductivity is strongly field dependent. At 4 K, the conductance increases by 8 orders of magnitude over one decade of bias. At a very high field, conductivity is temperature independent with $\sigma \sim \exp[-(E^*/E)^{1/2}]$. The complete behavior is very well described by variable range hopping with a Coulomb gap.

DOI: 10.1103/PhysRevLett.92.216802 PACS numbers: 73.22.–f, 05.60.Cd, 73.50.Fq, 73.63.Kv

Electron transport in amorphous semiconductors has been investigated for decades [1,2]. In recent years, "artificial solids" formed by close-packed arrays of monodispersed metallic nanostructures have provided novel model systems for the study of electron transport [3–5]. Semiconductor nanocrystals [6] can now be synthesized for a wide range of materials with nanometer sizes leading to strong quantum confinement. One of the best characterized systems is CdSe [7]. In several studies, neutral CdSe nanocrystal solids have been found to be photoconductive [8,9] but highly insulating [10]. Charging of the close-packed assemblies of the CdSe quantum dots (QDs) leads to vastly increased conductivity [11]. In this Letter, the electronic transport mechanism of CdSe *n*-type semiconductor nanocrystal solids is studied through temperature and field dependent dc-conduction experiments.

In a disordered insulator, Mott first pointed out that at low temperature the most frequent electron hopping among localized sites would not be to the nearest neighbor. Mott's variable range hopping model (M-VRH) gives the relation between conductance G and temperature T as [1]

$$G \propto \exp(-B/T^{\nu}) \tag{1}$$

with $\nu = 1/4$ for a 3D system, $\nu = 1/3$ for 2D. The essence of VRH can be summarized as below. A hopping electron will always try to find the lowest activation energy ΔE and the shortest hopping distance. There is an optimum hopping distance r, which maximizes the hopping probability. In zero bias condition, the probability is

$$P \sim \exp(-2r/a - \Delta E/k_{\mathrm{B}}T), \tag{2}$$

where a is the localization length, k_{B} is the Boltzmann constant, and ΔE is the activation energy.

Taking $\Delta E \sim 1/g_0 r^3$ (where g_0 is the density of states) and assuming a constant g_0 at the Fermi level, Mott derived a $\nu = 1/4$ law [1]. Considering the Coulomb interaction, Efros and Shklovskii (ES-VRH) showed that g_0 vanishes quadratically at the Fermi level and the conductance follows a $\nu = 1/2$ law [12]. In this model, the activation energy ΔE is proportional to $1/r$ as in the Coulomb potential, and it has a positive sign. In this Letter, we call ΔE "Coulomb barrier." However, this term is not the conventional Coulomb potential because it comes from a many body problem. It differs numerically from a Coulomb potential by a factor determined by computer simulation [2].

Above a certain critical temperature T_{C}, the Coulomb interaction can be neglected and the conductivity obeys Mott's law ($\nu = 1/4$) while below T_{C} the ES's $\nu = 1/2$ law holds [12]. T_{C} is given by

$$T_{\mathrm{C}} = \frac{e^4 a g_0}{k_{\mathrm{B}}(4\pi\varepsilon\varepsilon_0)^2}. \tag{3}$$

T_{C} is very small for usual amorphous materials. According to Knotek *et al.* [13], for amorphous Ge, $g_0 = 1.5 \times 10^{18}\ \mathrm{eV}^{-1}\,\mathrm{cm}^{-3}$, $a = 1$ nm, which gives $T_{\mathrm{C}} = 0.15$ K. In highly monodispersed semiconductor nanocrystals quantum confinement leads to discrete energy states with narrow homogeneous linewidth. If the overall linewidth is 100 meV and the radius of the QDs is ~3 nm, the density of states $g_0 \sim 9 \times 10^{19}\ \mathrm{eV}^{-1}\,\mathrm{cm}^{-3}$ is much larger than that for amorphous Ge. In QD arrays, the localization length is estimated by the radius of the dots, which is ~3 nm. Using an effective dielectric constant $\epsilon \sim 4$ for the close-packed CdSe QD films [14], T_{C} is estimated to be about 400 K in our samples, which means that the Coulomb gap plays an important role and the $\nu = 1/2$ law is expected.

The diameter of the nanocrystals is ~5.4 nm with a size variance of <5% and the interdot distance is ~0.7 nm. The nanocrystal films are made by drop-casting pyridine capped CdSe QDs solution on a Pt interdigitated working electrode with a 5 μm separation [11] corresponding to about 1000 diameters. The thickness of the film ranges from 10 to 50 layers of QDs and is determined by the optical density of the film. The film is then cross-linked by 1,4-phenylenediamine and baked

under N_2 at 70 °C for 2 h. This treatment helps achieve fast and robust charging of QDs [14]. The sample is further dried in vacuum overnight then immersed in anhydrous electrolyte solution (e.g., 0.1 M tetrabutylammonium tetrafluoroborate in *N, N*-dimethylformamide), which is sealed inside an electrochemical cell under nitrogen.

The CdSe nanocrystals are reduced by setting the working electrodes at a negative potential relative to a silver pseudoreference electrode [11]. Electrons are injected into the lowest quantum state, $1S_e$, as determined by optical measurements [11,14,15]. The conductance is measured by applying a fixed small bias between the two working electrodes. The sample is held at the negative potential while the electrochemical cell is cooled down in a liquid helium storage dewar. The temperature is read from a silicon diode embedded in the Teflon body of the electrochemical cell. When the electrolyte solution freezes (~200 K), the bipotentiostat is disconnected from the sample and the QD solids remain charged. The film conductance is stable for days when the sample is kept below ~160 K. At the same temperature, the *IV* curves are always the same no matter how long the sample stays at low temperature and how many times the sample is warmed up and cooled down. The frozen electrolyte solution does not contribute to the conduction. As a blank experiment, we measured the conductance of frozen electrolyte solution with the same interdigitated electrodes, which is undetectable (<1 pS) at all temperatures below 160 K.

IV curves are measured after the cell reaches thermal equilibrium. The *IV* curves are highly symmetric at all temperatures (Fig. 1) and show no hysteresis at the ramp rates used (~100 mV/s). The conductance drops as the temperature decreases (Fig. 2) and the *IV* curves are quite linear above 30 K. Below about 20 K, voltage thresholds appear above which the *IV* curves are extremely nonlinear [Fig. 3(b)].

To study the temperature dependent conductance at low bias, the film is cooled to 4 K then warmed up slowly (temperature increases at a rate of about 1 K/min) to maintain thermal equilibrium. The current is measured at a small bias of 1 V. The current is too small to detect (<1 pA) below 11 K, and the electrolyte solution starts to melt above 160 K. Between 11 and 120 K the conductance G (defined as $G = I/V$) follows very well the $\nu = 1/2$ law (Fig. 2)

$$G = A \exp\left(-\sqrt{\frac{T^*}{T}}\right). \tag{4}$$

The constant T^* is $\sim 5.2 \times 10^3$ K and A is $\sim 9.8 \times 10^{-3}$ S from the data fitting. The prefactor A includes tunneling through the high barrier created by the organic capping layers, and accounts for the attempt frequency of electrons trying to escape the nanocrystal.

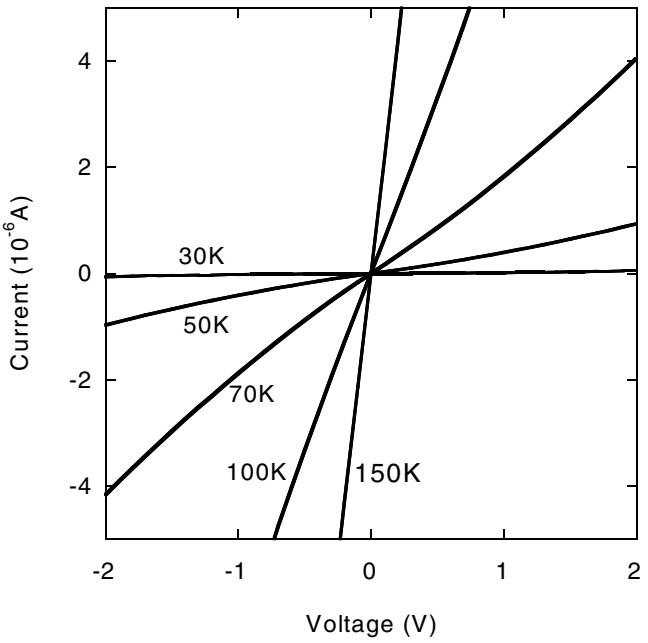

FIG. 1. Current-voltage (*IV*) curves for a typical *n*-type CdSe nanocrystal thin film. Above 30 K, *IV* curves are close to linear. Conductivity decreases as temperature decreases.

T^* is, in fact, predicted by the ES-VRH model [2],

$$T^* \approx \frac{2.8e^2}{4\pi\varepsilon\varepsilon_0 a k_B}. \tag{5}$$

Using the same values for the parameters as in the calculation of T_C, we obtained an expected $T^* = 3.9 \times 10^3$ K, which is in excellent qualitative agreement with the experimental value. ES-VRH over a smaller temperature range and with an even higher T^* has been recently reported for nanocrystalline $SiO_2/CdTe/SiO_2$ semiconductor films [16].

Above 120 K, the temperature dependence of the conductance starts to follow Arrhenius behavior (Fig. 2, inset). At these higher temperatures, Arrhenius behavior was previously reported in this system [11] as well as in ZnO nanocrystal assemblies [17]. In the VRH model, this happens when T is larger than T_A where nearest neighbor hopping is most favored. $T_A = (\frac{a}{4d})^2 T^*$ and d is the nearest neighbor distance. Using $T_A = 120$ K, one determines that the localization length is $a \sim 3.6$ nm, which is consistent with the earlier estimate. Achieving longer localization length requires reducing the barrier heights between the nanocrystals. Above T_A the conductance becomes thermally activated as $G = A \exp(-\frac{\Delta E_A}{k_B T})$ where the Arrhenius activation energy is $\Delta E_A = \frac{a}{8d} k_B T^* = 33$ meV. ΔE_A is about 30 meV as determined by data fitting indicating that the model is fully internally consistent. This is significantly smaller than the expected charging energy [18]. Indeed, using Eq. (5), $\Delta E_A \approx 0.35 E_C$, where $E_C = \frac{e^2}{4\pi\varepsilon\varepsilon_0 d}$ is a simple estimate of the charging energy.

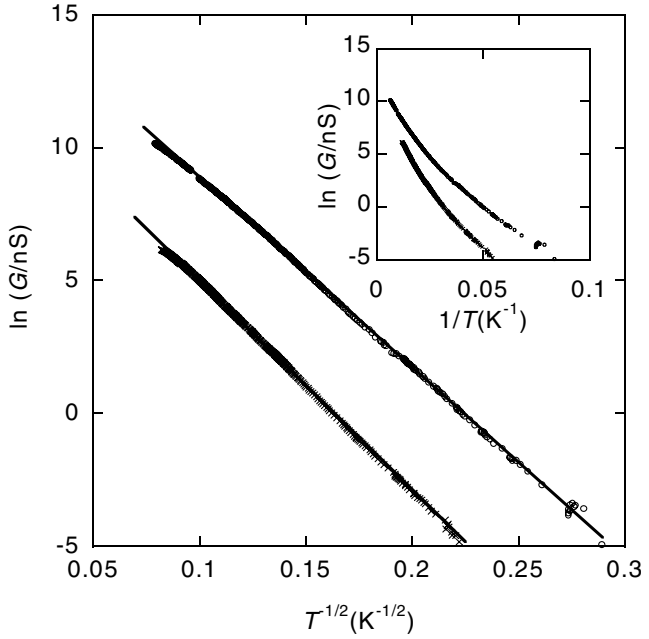

FIG. 2. Temperature dependence of the low-field conductance (bias = 1 V) in the range $11 < T < 160$ K. The two curves are the same sample at different charging levels. From fitting the data between 11 and 120 K, $T^* = 5.2 \times 10^3$ K (circle) and 6.2×10^3 K (cross). The inset plot is ln$G$ vs $1/T$ ($11 < T < 160$ K), where the conduction clearly deviates from Arrhenius behavior at low temperature.

The average number of electrons per dot was lowered by briefly melting the electrolyte at about 200 K. The film conductance dropped 10 times after this partial discharge but the temperature dependence still followed ES-VRH (Fig. 2, lower curve). The parameter T^* is a little larger ($\sim 6.2 \times 10^3$ K) in this case. The difference of T^* is probably due to the smaller localization length and reduced screening at lower doping level.

As discussed above, ES-VRH fits extremely well the data at low bias. However, at high bias the temperature dependence is strongly reduced, and one enters a regime where electron transport is field driven. The conductance increases by 8 orders of magnitude over one decade of bias at 4.3 K [Fig. 3(a)]. This extremely large dynamic range suggests the following modification of the hopping model. The down field energy is now reduced by eEr due to the electrical field E. Electron hopping is better facilitated when the voltage drop is of the order of the Coulomb barrier. We now write the hopping conductance to a nanocrystal downstream at a distance r as

$$G = A \exp\left(-2\frac{r}{a} - \frac{T^*}{T}\,\frac{a}{8r} + \frac{eEr}{k_B T}\right). \qquad (6)$$

When E is larger than a critical field $E_0 = \frac{2k_B T}{ea}$ (e.g., $E_0 = 2 \times 10^5$ V/m at 4 K), the conduction is field dominated. In this regime, the external field helps the electron overcome the Coulomb barrier, i.e., the last two terms in Eq. (6) cancel each other. This gives [19,20] a

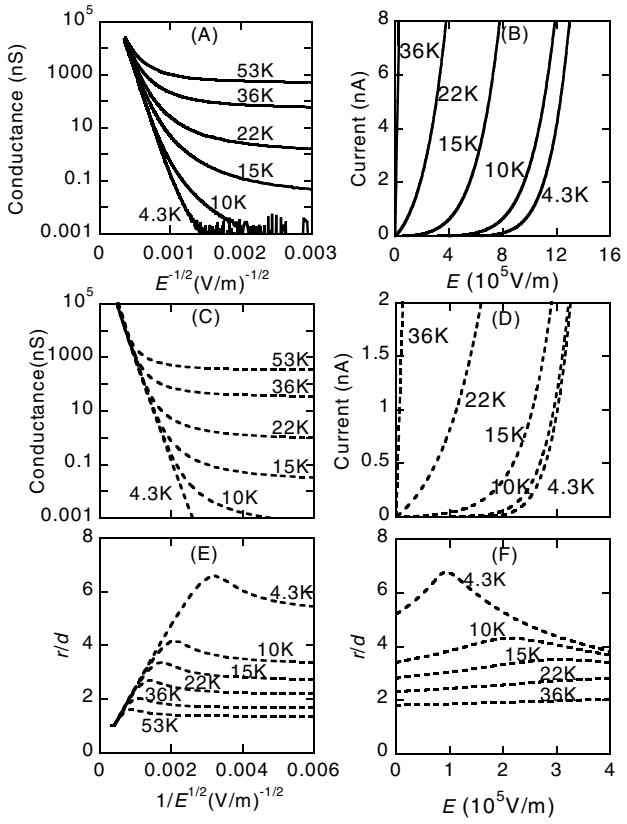

FIG. 3. Field dependence of conductivity. Solid lines are experimental data and dashes lines are from simulation. (a),(b) Experimental results with field strength range from 10^5 to 10^7 V/m. By fitting the linear part of the curve at 4.3 K in (a), $E^* = 3.4 \times 10^8$ V/m. (c)–(f) Simulation based on normalized variable range hopping model. r/d is the hopping distance scaled by the nearest neighbor distance d. For the simulation, the values of $A = 9.8 \times 10^{-3}$ S, $T^* = 5200$ K, and $a = 3.6$ nm from low field experiments are used.

temperature-independent conductance G,

$$G = A \exp\left(-\sqrt{\frac{E^*}{E}}\right), \qquad \text{where } E^* = \frac{k_B T^*}{2ea}. \qquad (7)$$

At higher bias, the conductance is strongly nonlinear and approaches Eq. (7) [Fig. 3(a)]. Using the same parameters as earlier, we calculated $E^* \sim 7.5 \times 10^7$ V/m. This is again in qualitative agreement with the experimental value of 3.4×10^8 V/m determined by fitting the data at the lowest temperature.

This nonlinearity is not likely due to the self-heating effect. We estimated the temperature difference across the thin glass substrate with thickness l (~ 2 mm) by

$$\Delta T = \frac{Pl}{\kappa S}, \qquad (8)$$

where P is the thermal power (<1 mW), κ is the thermal conductivity of the glass substrate (~ 2.5 mW/cm K), and S is the electrodes' area (~ 10 mm^2), we calculated the maximum temperature difference $\Delta T \sim 1$ K. Within the

experimental temperature range ($T > 4$ K), this difference can be neglected. In the measurements, the *IV* curves are independent of bias scan rate, and the rising and falling curves overlap very well. These observations provide supporting evidence that the self-heating effect is, indeed, insignificant.

To obtain a model that holds at all temperatures and field strengths, we modified Eq. (6) by normalizing the Boltzmann term by the partition function as below,

$$G = A \frac{\exp(-2\frac{r}{a} - \frac{T^*}{T}\frac{a}{8r} + \frac{eEr}{k_B T})}{1 + \exp(-\frac{T^*}{T}\frac{a}{8r} + \frac{eEr}{k_B T})} \quad (9)$$

with the same parameters as before.

At small E and T, Eq. (9) simplifies to (2), which leads to the $\nu = 1/2$ law and the experimental result at low bias (Fig. 2). When E becomes large, electrons most probably hop to the nearest neighbors and $r = d$ where d is the nearest neighbor distance. This tends to a temperature-independent conductance limit $A\exp(-2d/a)$.

The model is tested by simulations, in which we scanned r to maximize the conductivity in Eq. (9). Figures 3(c) and 3(d) demonstrate the resulting conductivity as a function of T, E, and Figs. 3(e) and 3(f) illustrate the hopping distance r scaled by the nearest neighbor distance d where the hopping distance first increases then decreases as the field becomes larger. The model reproduces very well the qualitative trend of the experimental data [Figs. 3(a)–3(d)] over many orders of magnitude by using the values of A, a, T^* experimentally determined as above. The details are not exactly the same. The critical field strength calculated is about 4 times weaker than the experimental value. Another difference is that the crossover between the Ohmic regime at low field and the temperature-independent regime at high field is somewhat softer in the experimental data than in the simulation [Fig. 3(a) and 3(c)]. However, given the simplicity of the model, the description is already surprisingly good.

CdSe nanocrystals with trioctylphosphine oxide (TOPO) capping molecules show similar conduction behavior although the conductivity is much smaller, possibly because the length of the TOPO ligand is longer than that of pyridine. The interdot distance increases from $\sim$0.7 nm for pyridine capped QDs to $\sim$1.1 nm in the case of TOPO capped QDs. We also doped the nanocrystal thin films n-type by potassium evaporation in an ultrahigh vacuum system [11]. The low temperature *IV* curves showed similar temperature and field dependent conductivity.

In summary, n-type semiconductor monodispersed QD solids exhibit very clearly variable range hopping where the energy barrier is dominated by the Coulomb interaction rather than by energy inhomogeneity. Over a wide temperature range (4–120 K) and fields up to 10^7 V/m, the variable range hopping model, with only three parameters, provides an excellent qualitative description of the conduction behavior over more than 8 orders of magnitude in current. Having developed an understanding for the CdSe system, parameters can now be identified and modified to reduce the temperature dependence of the conductivity and approach a more metallic behavior. Screening is one such experimentally adjustable parameter. Semiconductor nanocrystals made of materials with much larger dielectric constants should exhibit much weaker temperature dependence and possibly higher conductivity.

We acknowledge helpful discussions with H. M. Jaeger, I. Gruzberg, and T. F. Rosenbaum. D. Y. was supported by the University of Chicago–Argonne National Laboratory Consortium for Nanoscience Research. C. W. and B. L. W. were supported by the U.S. National Science Foundation (NSF) under Grant No. DMR-0108101. The use of the MRSEC Shared Facilities was supported by NSF under Grant No. DMR-0213745.

[1] N. F. Mott, J. Non-Cryst. Solids **1**, 1 (1968); N. F. Mott, *Conduction in Non-Crystalline Materials* (Clarendon Press, Oxford, 1993), 2nd ed.
[2] B. I. Shklovskii and A. L. Efros, *Electronic Properties of Doped Semiconductors* (Springer-Verlag, Berlin, 1984).
[3] R. C. Doty, H. Yu, C. K. Shih, and B. A. Korgel, J. Phys. Chem. B **105**, 8291 (2001).
[4] K. C. Beverly, J. F. Sampaio, and J. R. Heath, J. Phys. Chem. B **106**, 2131 (2002).
[5] R. Parthasarathy, X. M. Lin, and H. M. Jaeger, Phys. Rev. Lett. **87**, 186807 (2001).
[6] A. L. Efros and A. L. Efros, Sov. Phys. Semicond. **16**, 772 (1982).
[7] C. B. Murray, C. R. Kagan, and M. G. Bawendi, Annu. Rev. Mater. Sci. **30**, 545 (2000).
[8] C. A. Leatherdale *et al.*, Phys. Rev. B **62**, 2669 (2000).
[9] D. S. Ginger and N. C. Greenham, J. Appl. Phys. **87**, 1361 (2000).
[10] N. Y. Morgan *et al.*, Phys. Rev. B **66**, 075339 (2002).
[11] D. Yu, C. Wang, and P. Guyot-Sionnest, Science **300**, 1277 (2003).
[12] A. L. Efros and B. I. Shklovskii, J. Phys. C **8**, L49 (1975).
[13] M. L. Knotek *et al.*, Phys. Rev. Lett. **30**, 853 (1973).
[14] P. Guyot-Sionnest and C. Wang, J. Phys. Chem. B **107**, 7355 (2003).
[15] C. Wang, M. Shim, and P. Guyot-Sionnest, Science **291**, 2390 (2001).
[16] S. K. Bera, S. Chauduri, and A. K. Pal, Thin Solid Films **415**, 68 (2002).
[17] A. L. Roest, J. J. Kelly, and D. Vanmaekelbergh, Appl. Phys. Lett. **83**, 5530 (2003).
[18] A. Franceschetti, A. Williamson, and A. Zunger, J. Phys. Chem. B **104**, 3398 (2000).
[19] N. Apsley and H. P. Hughes, Philos. Mag. **31**, 1327 (1975).
[20] A. V. Dvurechenskii, V. A. Dravin, and A. I. Yakimov, JETP Lett. **48**, 155 (1988).